Proceedings of the 21st ICSMGE, Vienna, Austria, 14 – 19 June 2026. Pistrol, Adam & Schweiger (eds.)
Published by: ÖGG, Austrian Society for Geomechanics, Salzburg, Austria, ISBN 978-3-9503898-4-5
https://doi.org/10.53243/ICSMGE2026-1035

An anisotropic state-dependent elastic-viscoplastic multilaminate model for clays

Vahid Galavi
Witteveen+Bos, Rotterdam, The Netherlands, vahid.galavi@witteveenbos.com
Institute of Soil Mechanics and Foundation Engineering, TU Graz, Austria, vahid.galavi@tugraz.at

Helmut F. Schweiger
Institute of Soil Mechanics and Foundation Engineering, TU Graz, Austria

ABSTRACT: This paper presents a constitutive model within the multilaminate framework to describe the monotonic behaviour of clays. The model can intrinsically capture induced anisotropy of soils. The inherent anisotropy can be considered by applying independent parameters and state variables over sampling planes. Stress state and void ratio are considered as state variables. The mechanical behaviour of soil at any direction is a function of a 2-dimensional representation of the void ratio and stress state. A key feature of the model is its ability to simulate the rotation of principal stresses by automatically activating the sampling planes during the stress rotation. This capability makes the model suitable for modelling various geotechnical applications, such as the installation of piles, cone penetration testing (CPT), or the effect of the movement of trains and vehicles on soft embankments. Additionally, the model incorporates creep and viscosity effects to account for the rate-dependency observed in soft soils under various loading conditions.

KEYWORDS: Constitutive models, clay, multilaminate, anisotropy, viscoelasticity.

1 INTRODUCTION

To consider complex behavior of soils under various loading conditions, there has always been a need for advanced constitutive models in geotechnical engineering. The application of these models includes scenarios involving structures subjected to environmental loads, excavations, and transportation infrastructures such as roads and railways under traffic-induced stresses. In particular, clays exhibit several distinctive behaviors that are critical for realistic numerical predictions in such applications. These include rate dependency, induced and inherent anisotropy, principal stress rotation, and creep.

Among these, inherent anisotropy significantly influences the mechanical behavior, depending on the angle between the loading direction and the bedding plane formed during soil depositions (e.g. Schweiger et al., 2019). Induced anisotropy also plays an important role in the mechanical behavior of soils, especially in the application where a significant rotation of principal axis exists, such as embankments, excavations and moving loads on roads and railways. The material anisotropy becomes particularly pronounced at large strain, leading to variations in strengths, stiffnesses, and dilatancy characteristics (Schädlich & Schweiger, 2012). Understanding of these factors is important for improving the accuracy of numerical models used to address geotechnical challenges in saturated clayey natural deposits.

The accuracy of material models depends on their capabilities and the incorporated features. Discovering a single model able to capture all relevant features is rare. Furthermore, the addition of features typically increases the number of material parameters, complicating both the formulation and calibration processes.

A class of constitutive models which can intrinsically incorporate induced anisotropy and rotational principal stresses without excessive mathematical complexity, are formulated within the multilaminate framework. This framework establishes a simplified relationship between the microscale and macroscale mechanical behavior of materials. It is based on the slip theory of Taylor (1938), which was extended by Batdorf & Budiansky (1949) and Sanders (1955) for modeling plastic behavior of metals. Zienkiewicz & Pande (1977) applied this framework to simulate mechanical behavior of jointed rocks using a certain number of predefined planes of joints. Later, Pande & Sharma (1983) formulated an elasto-plastic model for clays within this framework, and Sadrnejad & Pande (1989) applied it to sands.

Wiltafsky (2003) introduced a multilaminate model for clays within the double hardening framework. Galavi (2007) extended it to include inherent anisotropy by defining different strength parameters over sampling planes using a microstructure tensor proposed by Pietruszczak & Mroz (2000). Schädlich (2012) further enhanced the model with an anisotropic small strain formulation to capture both strength and stiffness anisotropy. However, these models lacked state-dependency and required separate calibration for different soil states.

State-dependent multilaminate models for sands were developed recently in several studies. Dashti et al. (2019) developed a model based on the bounding surface plasticity of Dafalias & Manzari (2004). Bayraktaroglu et al. (2024) developed a novel anisotropic model by implementing the anisotropic critical state theory of Li & Dafalias (2012) in the multilaminate framework.

To the best of authors' knowledge, no state-dependent multilaminate model has yet been developed for clays. This study introduces MultiClay, a state-dependent multilaminate model for clays that captures inherent and induced anisotropy, rotation of principal stresses, creep and rate-dependency. The model builds on the DeltaSand model (Galavi, 2021), originally developed for isotropic sands under monotonic and cyclic loadings. Like DeltaSand, MultiClay is capable of simulating cyclic loadings, although this aspect is not addressed here.

A key feature of the model is its ability to simulate the rotation of principal stresses by automatically activating the sampling planes during the stress rotation, making it well-suited for modelling a variety of geotechnical applications, such as pile installation, cone penetration testing (CPT), excavations, and the effects of moving traffic on soft embankments.

After describing the formulation of the model, it is validated against the experimental data of a Kaolin clay (Wichtmann & Triantafyllidis, 2017).

2 FORMULATION

2.1 *Multilaminate*

The multilaminate framework establishes a simplified relationship between the microscale and macroscale mechanical behavior of materials. A similar approach, called microplane framework, was developed by Bažant & Oh (1983) for modeling behavior of concrete and rocks. The basic principles and formulations of these two frameworks are reviewed and discussed in detail in Sanchez et al. (2008). The main difference between the multilaminate and microplane models is the projection of macroscopic stress or microscopic strain to sampling planes. In the multilaminate the macroscopic stresses are projected to sampling planes to calculate microscopic plastic strains and update the macroscopic stresses from the integrated microscopic plastic strains, whereas the microplane models project macroscopic strains to calculate microplane stresses to obtain a stress-strain relationship from integrated microplane stresses.

In the current study, another type of multilaminate framework is examined, in which the trial macroscopic stresses are first calculated using elasticity theory and then projected to sampling planes to obtain elasto-viscoplastic microscopic stresses. The macroscopic elasto-viscoplastic behavior is then obtained by the integration of microscopic stresses.

The trial effective stress tensor, $\boldsymbol{\sigma}^{tr}$, is calculated using the elastic stiffness, $\mathbf{D}^{e}$, and the increment of strain, $\mathbf{d\varepsilon}$, as follows:

$$\boldsymbol{\sigma}^{tr} = \mathbf{D}^{e}\mathbf{d\varepsilon} + \boldsymbol{\sigma_0} \tag{1}$$

in which $\boldsymbol{\sigma_0}$ is the macroscopic effective stress tensor from the previous calculation step. The trial effective stress tensor is projected to each sampling plane using the normal unit vector of planes. The microscopic effective stress on sampling plane *i* can be expressed as follows:

$$\boldsymbol{\sigma}_i^{tr} = \begin{bmatrix}\sigma_n^{tr}\\ \tau^{tr}\end{bmatrix} = \begin{bmatrix}\boldsymbol{\sigma}^{tr}\boldsymbol{n_i}\cdot\boldsymbol{n_i}\\ \|\boldsymbol{\sigma}^{tr}\boldsymbol{n_i} - (\boldsymbol{\sigma}^{tr}\boldsymbol{n_i}\cdot\boldsymbol{n_i})\boldsymbol{n_i}\|\end{bmatrix} \tag{2}$$

$\boldsymbol{n_i}$ is the unit vector of sampling plane *i*. The microscopic stress, $\boldsymbol{\sigma}_i^{tr}$, is corrected independently on each sampling plane using its state variables and the microscopic stress-strain relationship to obtain an elasto-plastic microscopic stress, $\boldsymbol{\sigma}_i$. The microscopic elasto-viscoplastic relationships are described in the following sections. The macroscopic elasto-viscoplastic stress is then calculated by integrating the microscopic stresses as follows:

$$\boldsymbol{\sigma} = 3\sum_{i=1}^{n_{SP}} \boldsymbol{\sigma}_i \mathbf{T_i} w_i \tag{3}$$

or

$$\boldsymbol{\sigma} = 3\sum_{i=1}^{n_{SP}} \left(\sigma_{n,i}\left(\frac{\partial\sigma_n}{\partial\boldsymbol{\sigma}}\right)_i + \tau_i\left(\frac{\partial\tau}{\partial\boldsymbol{\sigma}}\right)_i\right) w_i \tag{4}$$

in which $\mathbf{T_i}$ is the transformation matrix from local to global (microscopic to macroscopic) systems, and w_i is the weight of sampling plane *i*. Bažant & Oh (1985) calculated normal unit vectors and weights of sampling planes for different number of planes per unit sphere, ranging from 2x21 to 2x61 planes. The transformation matrix has the following components:

$$\left(\frac{\partial\sigma_n}{\partial\boldsymbol{\sigma}}\right)_i = \begin{bmatrix} n_1\cdot n_1\\ n_2\cdot n_2\\ n_3\cdot n_3\\ n_1\cdot n_2\\ n_2\cdot n_3\\ n_3\cdot n_1\end{bmatrix}_{\boldsymbol{i}} \tag{5}$$

and

$$\left(\frac{\partial\tau}{\partial\boldsymbol{\sigma}}\right)_i = \begin{bmatrix} \dfrac{n_1\cdot(\boldsymbol{\sigma}^{tr}\boldsymbol{n}_i)_1 - \sigma_n^{tr}n_1\cdot n_1}{\tau^{tr}}\\ \dfrac{n_2\cdot(\boldsymbol{\sigma}^{tr}\boldsymbol{n}_i)_2 - \sigma_n^{tr}n_2\cdot n_2}{\tau^{tr}}\\ \dfrac{n_3\cdot(\boldsymbol{\sigma}^{tr}\boldsymbol{n}_i)_3 - \sigma_n^{tr}n_3\cdot n_3}{\tau^{tr}}\\ \dfrac{n_2\cdot(\boldsymbol{\sigma}^{tr}\boldsymbol{n}_i)_1 + n_1\cdot(\boldsymbol{\sigma}^{tr}\boldsymbol{n}_i)_2 - 2\sigma_n^{tr}n_1\cdot n_2}{2\tau^{tr}}\\ \dfrac{n_3\cdot(\boldsymbol{\sigma}^{tr}\boldsymbol{n}_i)_2 + n_2\cdot(\boldsymbol{\sigma}^{tr}\boldsymbol{n}_i)_3 - 2\sigma_n^{tr}n_2\cdot n_3}{2\tau^{tr}}\\ \dfrac{n_1\cdot(\boldsymbol{\sigma}^{tr}\boldsymbol{n}_i)_3 + n_3\cdot(\boldsymbol{\sigma}^{tr}\boldsymbol{n}_i)_1 - 2\sigma_n^{tr}n_3\cdot n_1}{2\tau^{tr}}\end{bmatrix}_{\boldsymbol{i}} \tag{6}$$

As can be seen the transformation matrix is based on the direction of trial stress. Therefore, to minimize the error in this method, the increment of the trial stress should be limited, which is ensured in the proposed model by means of a sub-stepping scheme. In material with low stiffness, such as clays, the sub-stepping scheme does not have a significant effect on the performance of the model. In the current model, the maximum deviatoric strain is limited to 0.01% in each calculation step.

2.2 *Microscopic formulation of material model*

The visco-plastic model is formulated based on the double-hardening DeltaSand model for sands (Galavi, 2021). In this framework separate yield surfaces are used for certain loading conditions. In the context of multilaminate framework, surfaces are defined as lines on sampling planes. Therefore, the term yield or plastic potential lines are used in the following sections. Similar to DeltaSand, two isotropic hardening yield lines for monotonic loadings and two kinematic lines for cyclic loadings are considered. The present paper focuses on monotonic loadings and therefore the formulation of the kinematic hardening parts is omitted. Figure 1 shows the yield lines of the model for monotonic loadings.

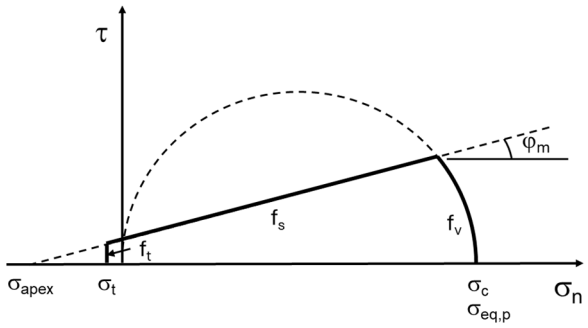

Figure 1. Isotropic hardening yield lines of the model.

2.3 *Local void ratio*

State-dependency on sampling planes is formulated using a local void ratio concept. In the beginning of the simulation, the global void ratio, e_g, is transformed to sampling planes and stored as local void ratios on individual planes. For the transformation, it can be assumed that the initial local void ratio is isotropic or anisotropic. The anisotropic void ratio can be

considered using the microstructure tensor, proposed by Pietruszczak & Mroz (2000). This concept was later applied to the multilaminate framework to model inherent anisotropy of strength parameters (Pietruszczak & Pande, 2001, Cudny & Vermeer, 2004, Galavi, 2007, Schweiger et al., 2009).

The local void ratio, e_l, on sampling plane i is updated using the increment of the normal strain of the same plane, $d\varepsilon_n$, as:

$$e_l = (1 + e_{l,0})\exp(-d\varepsilon_n) - 1 \tag{7}$$

in which $e_{l,0}$ is the local void ratio in the beginning of the step.

2.4 *Shear part*

The shear part of the model is formulated with a Mohr-Coulomb line on a sampling plane by introducing mobilized friction angle φ_m:

$$f_s = \tau - (\sigma_n - \sigma_{apex}) \tan \varphi_m \tag{8}$$

where τ and σ_n are the shear and normal stresses on the sampling plane. The apex stress is defined as a function of cohesion, c, and critical friction angle, φ_{cv}:

$$\sigma_{apex} = c \cot \varphi_{cv} \tag{9}$$

The hardening rule of Pietruszczak and Niu (1992) with the modification of Wan and Guo (1998) is used to define the mobilized friction angle as a function of shear plastic strain, γ^p, and void ratio, e_l:

$$\tan \varphi_m = \tan \varphi_i + \frac{\gamma^p f_d(e_l)}{A_{mat} + \gamma^p} (\tan \varphi_{cv} - \tan \varphi_i) \tag{10}$$

in which φ_i' is the initial friction angle on the sampling plane from which the mobilization starts. This friction angle is calculated based on the initial stresses during the initialization of the model. A_{mat} is an input parameter that defines the plastic behaviour of soil during shearing. A higher value of A_{mat} leads to a softer response and, consequently, more plastic strains.

The function $f_d(e_l)$ relates the hardening (or softening) rule to the local void ratio and is defined as follows (Wan & Guo, 1998):

$$f_d(e) = \left(\frac{e_l}{e_{cr}}\right)^{-\alpha} \tag{11}$$

in which e_{cr} is the critical void ratio and α is a non-negative input parameter. In the current formulation, it is assumed that the critical void ratio is isotropic and has the same value for all sampling planes. For void ratios greater than the critical void ratio (normally consolidated clays), f_d is less than 1 and for void ratios less than the critical void ratio (over-consolidated clays), f_d is greater than 1. At the critical state, when the void ratio tends to 1, f_d becomes 1.

2.4.1 *Flow rule*

A non-associated Mohr-Coulomb type of plastic potential function is used:

$$g_s = \tau - \sigma_n \tan \psi_m \tag{12}$$

in which ψ_m is the mobilized dilation angle. Using the stress-dilatancy theory of Rowe and modification proposed by Wan & Guo (1998) for sands, the following relationship can be derived between the mobilized dilation and friction angles:

$$\tan \psi_m = \tan \varphi_m - f_e(e) \tan \varphi_{cv} \tag{13}$$

φ_{cv} is the critical void ratio and $f_e(e)$ is a function to incorporate the void ratio in the evolution of strain (Wan & Guo, 1998):

$$f_e(e) = F_f \left(\frac{e_l}{e_{cr}}\right)^{\beta} \tag{14}$$

β is an input parameter to define dilation of material during shearing as a function of void ratio. For mobilized friction angles lower than 0.75 $\tan \varphi_{cv}$, the function $f_e(e)$ is multiplied by the following factor to obtain more contractive behaviour in the beginning of shearing as observed in clays.

$$F_f = \frac{4}{3}(1 - f_f)\left(\frac{\tan \varphi_m}{\tan \varphi_{cv}}\right) + f_f \tag{15}$$

In which f_f is an input parameter, defining initial fabric of the material.

2.4.2 *Rate-dependent shearing*

The rate-dependent (viscous) behavior of the shear part is formulated using the Perzyna overstress theory. According to the theory of visco-plasticity, the total strain rate tensor, $\dot{\boldsymbol{\varepsilon}}$, is summation of the elastic and visco-plastic strain rate tensors:

$$\dot{\boldsymbol{\varepsilon}} = \dot{\boldsymbol{\varepsilon}}^e + \dot{\boldsymbol{\varepsilon}}^{vp} \tag{16}$$

The elastic strain rate tensor can be related to the stress tensor using the elastic stiffness, i.e.:

$$\dot{\boldsymbol{\sigma}} = \mathbf{D}^e \dot{\boldsymbol{\varepsilon}}^e \tag{17}$$

The visco-plastic strain rate is given by:

$$\dot{\boldsymbol{\varepsilon}}^{vp} = \dot{\lambda} \frac{\partial g_s}{\partial \boldsymbol{\sigma}} = \frac{1}{\mu} \langle \Phi(f_s) \rangle \mathbf{D}^e \dot{\boldsymbol{\varepsilon}}^e \tag{18}$$

where $\langle ... \rangle$ is McCauley brackets, which represent a function that is zero when its argument is negative and equal to the argument itself when it is positive or zero. μ is the viscosity-related input parameter which is material, temperature, stress and strain rate dependent. $\Phi(f_s)$ is an overstress function of yield function and needs to be defined based on experimental data. The most widely used overstress function is defined according to Perzyna overstress model as:

$$\Phi(f) = \left(\frac{f_s}{f_0}\right)^n \tag{19}$$

where n is the rate sensitivity parameter, f_s is yield function of the shear part of the model and f_0 is a reference normalization yield stress.

2.5 *Volumetric part*

The volumetric yield line of the model has an elliptical shape, the same as the modified Cam-Clay surface which expands isotopically with plastic normal strains. The volumetric yield line is expressed by:

$$f_v = \frac{\tau^2}{M_v} + \sigma_n(\sigma_n - \sigma_c) \tag{20}$$

σ_c is the pre-consolidation stress. M_v is a shape parameter which affects K_0 stress paths in normally consolidation loading. In the current model M_v is calculated internally from the input parameter K_0^{nc} and elasticity parameters as given in Brinkgreve (1994).

An associated hardening rule is considered for volumetric part. The pre-consolidation stress, σ_c, increases with increasing

normal plastic strain, $d\varepsilon_n^p$. When creep is neglected, the pre-consolidation pressure can be obtained from:

$$\sigma_c = \sigma_{c,0}\exp\left(\frac{(1+e_{l,0})d\varepsilon_n^p}{\lambda-\kappa}\right) \quad (21)$$

where $\sigma_{c,0}$ is the pre-consolidation pressure in the beginning of the step. The slope of the normal compression line, λ, and the slope of the unloading-reloading lines, κ, in $e-\ln\sigma_n$ space is obtained from the following relationships:

$$\kappa = \frac{3(1+e_{l,0})(1-2\upsilon_{ur})}{2G^{ref}(1+\upsilon_{ur})}\sigma_n\left(\frac{\sigma_n+\sigma_{apex}}{\sigma_{ref}+\sigma_{apex}}\right)^{-m} \quad (22)$$

and

$$\lambda = \frac{(1+e_{l,0})}{E_{oed}^{ref}}\sigma_n\left(\frac{\frac{\sigma_n}{K_0^{nc}}+\sigma_{apex}}{\sigma_{ref}+\sigma_{apex}}\right)^{-m} \quad (23)$$

G^{ref} and E_{oed}^{ref} represent the reference shear and oedometer stiffnesses, respectively. υ_{ur}, σ_{ref} and m are the unload/reload Poisson's ratio, the reference stress (usually taken as 100 kPa) and the stiffness power, respectively.

For most clays, the power parameter m can be taken as 1. In this case, by considering no cohesion, i.e. $\sigma_{apex}=0$, the above equations can be simplified as follows in the multilaminate model which are slightly different from the equations derived for 3D models:

$$\kappa = \frac{3(1+e_{l,0})(1-2\upsilon_{ur})}{2G^{ref}(1+\upsilon_{ur})}\sigma_{ref} \quad (24)$$

and

$$\lambda = \frac{(1+e_{l,0})}{E_{oed}^{ref}}\sigma_{ref}K_0^{nc} \quad (25)$$

2.5.1 *Creep*

The rate-dependent behavior of the volumetric part is formulated based on the 3D creep model proposed by Vermeer & Neher (1999), which was an extension of the one-dimensional creep model of Bjerrum. According to this model, the pre-consolidation stress depends entirely on the amount of creep strain accumulated in time. The total strain rate tensor, $\dot{\boldsymbol{\varepsilon}}$, is summation of the elastic and creep strain rate tensors:

$$\dot{\boldsymbol{\varepsilon}} = \dot{\boldsymbol{\varepsilon}}^e + \dot{\boldsymbol{\varepsilon}}^c \quad (26)$$

in which $\dot{\boldsymbol{\varepsilon}}^c$ is the creep strain rate tensor. Following the work of Vermeer & Neher (2000), it can be shown that the normal creep strain rate on a sampling plane can be calculated from:

$$\dot{\varepsilon}_n^c = \frac{\mu^*}{\tau_t}\left(\frac{\sigma_{eq}}{\sigma_{eq,p}}\right)^{\frac{\lambda-\kappa}{\mu^*(1+e_{l,0})}} \quad (27)$$

In which $\mu^*$and τ_t are creep and time parameters. In standard oedometer tests, τ_t is equal to one day. In the proposed model, τ_t is an input parameter. The creep parameter, μ^*, is specified using an input parameter, μ_f, as a factor of λ, defined as follows:

$$\mu^* = \mu_f\lambda \quad (28)$$

$\sigma_{eq,p}$ is a generalized pre-consolidation stress, in case creep is activated in the model (when the creep parameters are provide). Using a similar equation as the one used for the non-creep model (Eq. (21)), $\sigma_{eq,p}$ can be obtained:

$$\sigma_{eq,p} = \sigma_{eq,p,0}\exp\left(\frac{(1+e_{l,0})d\varepsilon_n^c}{\lambda-\kappa}\right) \quad (29)$$

The total strain rate is derived by Vermeer & Neher (2000) as follows:

$$\dot{\boldsymbol{\varepsilon}} = \mathbf{D}^{e-1}\dot{\boldsymbol{\sigma}} + \frac{\dot{\varepsilon}_n^c}{\alpha}\frac{\partial\sigma_{eq}}{\partial\sigma} \quad (30)$$

and

$$\alpha = \frac{\partial\sigma_{eq}}{\partial\sigma_n} \quad (31)$$

The equivalent stress can be obtained using the volumetric yield function as follows:

$$\sigma_{eq} = \frac{\tau^2}{M_v\sigma_n} + \sigma_n^2 \quad (32)$$

2.6 *Tension cut-off*

The tension cut-off yield line is defined as follows:

$$f_t = \sigma_t - \sigma_n \quad (33)$$

in which σ_t is the input tensile strength ($\sigma_t \le \sigma_{apex}$).

2.7 *Elastic behavior*

The elastic behavior of the model is defined globally. An extended Masing rule defines the small strain stiffness of the material during unloading and reloading. The reference shear stiffness, G^{ref}, is expressed by means of the modified Hardin and Drnevich relationship (Santos & Correria, 2001):

$$G^{ref} = \frac{G_0^{ref}}{1+a\left(\frac{\gamma}{\gamma_r}\right)} \quad (34)$$

in which G_0^{ref} is the initial reference shear stiffness (small strain stiffness), γ is the shear strain. γ_r and a are two input parameters. The parameter a can be taken as 0.385 so that γ_r is defined as the reference shear strain at which G^{ref} is reduced to $0.722G_0^{ref}$. It should be noted that the reference shear stiffness cannot be reduced to values lower than the unloading-reloading reference stiffness, G_{ur}^{ref}, specified as an input parameter.

The current stiffness is calculated considering the stress-dependency of the stiffness as follows:

$$G = G^{ref}\left(\frac{p}{\sigma_{ref}}\right)^m \quad (35)$$

in which p is the global mean effective stress.

2.8 *Input parameters*

The proposed model consists of several features, such as viscosity, creep, cyclic behavior and small strain stiffness which can separately be switched off. In this study, the cyclic behavior of the model is omitted. The list of parameters is presented in Table 1.

3 VALIDATION

The proposed material model is validated against experimental data of a Kaolin clay (Wichtmann & Triantafyllidis, 2017). The Kaolin clay is a low plasticity reconstituted clay. The calibrated parameters of the material model are presented in Table 1. The oedometer test with different loading, unloading and reloading steps under different strain rates is plotted in Figure 2. The loading rates are based on the values provided in Fuentes et al. (2018). Figure 3 shows results of one-dimensional CRS (Constant Rate of Strain) test. Soil samples with slightly different initial void ratios are compressed at various strain rates. As can be seen from these tests that the model is capable of capturing various loading conditions with different strain rates with good accuracy.

Table 1. Input parameters of the proposed model calibrated for Kaolin clay.

Parameter	Symbol	Value	Unit
Reference unloading-reloading stiffness	E_{ur}^{ref}	5000	kPa
Reference oedometer stiffness	E_{oed}^{ref}	1200	kPa
Poisson's ratio	υ_{ur}	0.15	-
Power stiffness parameter	m	0.7	-
Normal-consolidation stress coefficient	K_0^{nc}	0.6157	-
Critical state friction angle	φ_{cv}	22.6	degrees
Effective cohesion	c	1.0	kPa
Critical void ratio	e_{cr}	1.72	-
Controlling peak friction angle	α	0.0	-
Controlling dilation	β	0.0	-
Controlling plasticity	A_{mat}	0.01	-
Tensile strength	σ_t	0.0	kPa
Small strain ratio	G_0/G	5	-
Reference small strain	γ_r	0.0001	-
Creep coefficient	μ_f	0.015	-
Creep time parameter	τ_t	1	day
Initial fabric parameter	f	5	-
Number of sampling planes	n_{SP}	37	-

Simulations of undrained triaxial tests are presented in Figure 4 and Figure 5. All these tests were conducted with a rate-independent material model, i.e. no viscosity or creep is considered. Figure 3 shows deviatoric stress versus axial strain. As can be seen, the model captures the mechanical behavior of the Kaolin clay at different confining stress with one set of parameters. The corresponding stress path in p-q space is plotted in Figure 5. The critical state line, obtained from the experiments, is curved, which is simplified in the model by considering a linear critical state line. This results in a slight underestimation of the maximum deviatoric stresses at confining stresses of 50 kPa and 200 kPa. Overall, the predictions are in good agreement with experimental tests.

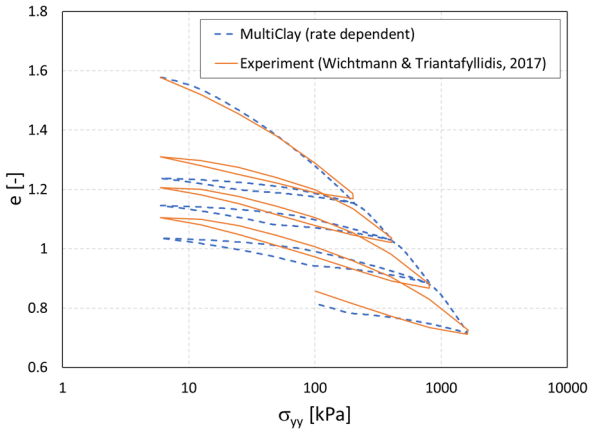

Figure 2. Void ratio versus vertical stress in oedometer test with loading, unloading-reloading steps.

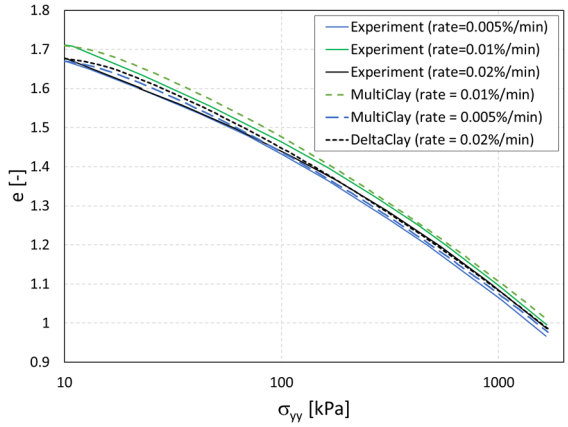

Figure 3. Void ratio versus vertical stress in CRS test with different loading rates.

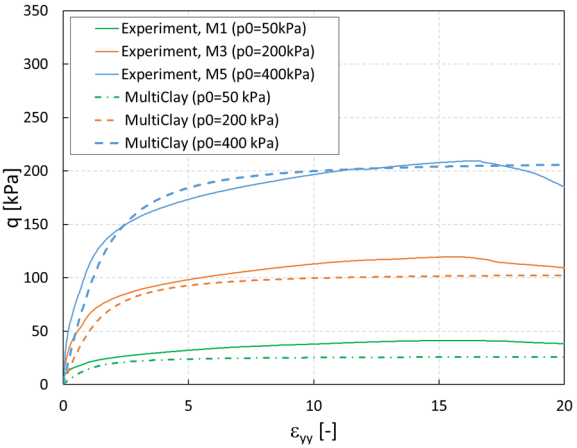

Figure 4. Deviatoric stress versus axial strain in undrained triaxial test.

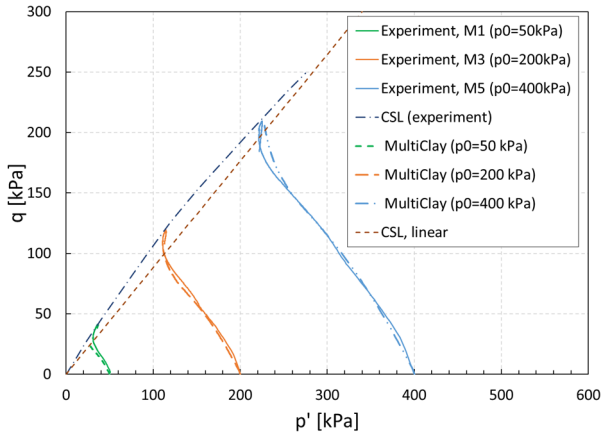

Figure 5. Deviatoric stress versus mean effective stress in undrained triaxial test.

4 CONCLUSIONS

In this paper the formulation of a state-dependent constitutive model for clays is presented. The model was formulated within the framework of multilaminate, which provides a basis to account induced anisotropy and rotation of principal axes. Inherent anisotropy can be introduced to the model by defining different parameters over individual sampling planes. In addition to anisotropy, the proposed model incorporates creep and rate-dependency. The constitutive model was validated against oedometer and triaxial tests on Kaolin clay. The results show a good agreement between the numerical and experimental results. In future studies, the performance of the model against cyclic loadings on clays will be demonstrated.

5 REFERENCES

Batdorf, S. B., and Budiansky, B. 1949. A mathematical theory of plasticity based on the concept of slip. Rep. No. TN 1871, National Advisory Committee for Aeronautics, Washington, D.C.

Bayraktaroglu, H., Hicks, M.A., Korf, M., and Galavi V. 2024. A state-dependent multilaminate constitutive model for anisotropic sands. Geotechnique, 74(12):1343–1359.

Bažant, Z. P., and Oh, B. H. 1983. Microplane model for fracture analysis of concrete structures. Proc., Symp. on the Interaction ofNon-Nuclear Munitions with Structures, C. A. Ross, ed., U.S. Air Force Academy, Colorado Springs, McGregor & Werner, Inc., Washington, D.C., 49–55.

Bažant, Z. P., and Oh, B. H. 1985. Microplane model for progressive fracture of concrete and rock. J. Eng. Mech., 111(4), 559–582.

Brinkgreve, R. B. J. 1994. *Geomaterial models and numerical analysis of softening*. Ph.D. thesis, Delft Univ. of Technology, Delft, The Netherlands.

Cudny, M., and Vermeer, P. A. 2004. On the modelling of anisotropy and destructuration of soft clays within the multilaminate framework. Comput. Geotech. 31, No. 1, 1–22.

Dafalias YF, and Manzari MT. 2004. Simple plasticity sand model accounting for fabric change effects. J Eng Mech, 130, 622–34.

Dashti, H., Sadrnejad, S.A., and Ganjian, N. 2019. A novel semi-micro multilaminate elasto-plastic model for the liquefaction of sand. Soil Dynamics and Earthquake Engineering, 124, 121-135.

Fuentes, W., Tafili, M., and Triantafyllidis, Th. 2018. An ISA-plasticity-based model for viscous and non-viscous clays. Acta Geotechnica, 13, 367-386.

Galavi, V. 2007. *A multilaminate model for structured clay incorporating inherent anisotropy and strain softening*. Ph.D. thesis, Graz Univ. of Technology, Graz, Austria.

Galavi, V. 2021. DeltaSand: A state-dependent double hardening elasto-plastic model for sand: formulation and validation. Comput. Geotech. 129, 103844.

Li, X. S. and Dafalias, Y. F. 2012. Anisotropic critical state theory: role of fabric. J. Engng Mech. 138, No. 3, 263–275.

Vermeer, P.A., and Neher, H.P. 1999. A soft soil model that accounts for creep. Beyond 2000 in Computational Geotechnics. 1-13.

Pande, G. N., and Sharma, K. G. 1983. Multilaminate model of clays—A numerical evaluation of the influence of rotation of principal stress axes. Int. J. Numer. Analyt. Meth. Geomech., 7(4), 397–418.

Pietruszczak, S., and Pande, G. N. 2001. Description of soil anisotropy based on multilaminate framework. Int. J. Numer. Anal. Meth. Geomech. 25, No. 2, 197–206.

Pietruszczak, S., and Mroz, Z. 2000. Formulation of anisotropic failure criteria incorporating a microstructure tensor. Comput. Geotech. 26, No. 2, 105–112.

Pietruszczak, S., and Niu, X. 1992. Numerical evaluation of bearing capacity of a foundation in strain softening soil. Comput. Geotech., 13(3), 187–198.

Sadrnejad, S. A., and Pande, G. N. 1989. A multilaminate model for sands. Proc., 3rd Int. Symp. on Numerical Models in Geomechanics (NUMOG), S. Pietruszczak and G. N. Pande, eds., Elsevier Science, New York, 17–27.

Sánchez, F., Prat, P. C., Galavi, V., and Schweiger, H. F. 2008. Multilaminate and microplane models: Same principles and different solutions for constitutive behaviour of geomaterials. Proc., 12th Int. Conf. of Int. Association for Computer Methods and Advances in Geomechanics (IACMAG), Indian Institute of Technology, Goa, India, 911–919.

Sanders, J. L. 1955. Plastic stress-strain relations based on linear loading functions. Proc., 2nd United States National Congress on Applied Mechanics, ASME, New York, 455–460.

Santos, J., and Correia, A., 2001. Reference threshold shear strain of soil. its application to obtain a unique strain-dependent shear modulus curve for soil. In: 15th International Conference SMGE, Istanbul, Turkey, 267–270.

Schädlich, B. 2012. *A multilaminate constitutive model for stiff soils*. Ph.D. thesis, Graz Univ. of Technology, Graz, Austria.

Schädlich, B., and Schweiger H.F. 2012. A multilaminate constituitve model accounting for anisotropic small strain stiffness. Int. J. Nummer. Anal. Mech. Geomech., 37(10), 1337–1362.

Schweiger H.F., Wiltafsky C, Scharinger F, and Galavi V. 2009. A multilaminate framework for modelling induced and inherent anisotropy of soils. Geotechnique, 59(2), 87–101.

Taylor, G. I. 1938. Plastic strain in metals: Journal of the institute of metals. The Scientific Papers of G. I. Taylor 1, 1958, Vol. 62, Cambridge University, Cambridge, U.K., 307–324.

Wan, R.G., and Guo, P.J., 1998. A simple constitutive model for granular soils: modified stress-dilatancy approach. Comput. Geotech. 22, 109–133.

Wichtmann, T., Triantafyllidis, T., 2017. Monotonic and cyclic tests on kaolin: a database for the development, calibration and verification of constitutive models for cohesive soils with focus to cyclic loading. Acta Geotechnica 13(5):1103-1128, DOI 10.1007/s11440-017-0588-3.

Wiltafsky, Ch. 2003. *A multilaminate model for normally consolidated clay*. Ph.D. thesis, Graz Univ. of Technology, Austria.

Zienkiewicz, O. C., and Pande, G. N. 1977. Time-dependent multilaminate model of rocks—A numerical study of deformation and failure of rock masses. Int. J. Numer. Analyt. Meth. Geomech., 1(3), 219–247.